Article

Unusual Chemistry of the Complex Mg(2-Fluoropyridine) Activated by the Photoexcitation of Mg

Hai-Chuan Liu, Shihe Yang, Xin-Hao Zhang, and Yun-Dong Wu

J. Am. Chem. Soc., **2003**, 125 (40), 12351-12357• DOI: 10.1021/ja036476a • Publication Date (Web): 13 September 2003

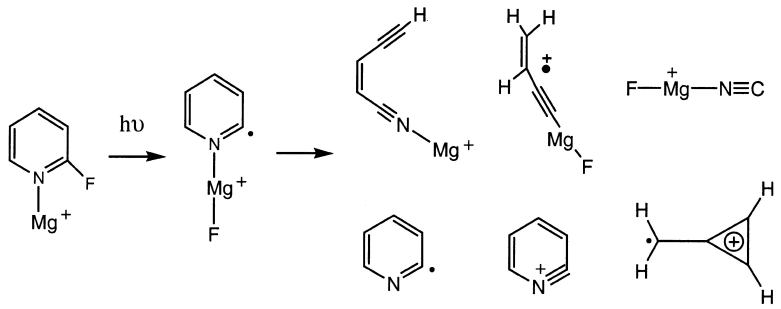

More About This Article

Additional resources and features associated with this article are available within the HTML version:

- Supporting Information
- Links to the 1 articles that cite this article, as of the time of this article download
- Access to high resolution figures
- Links to articles and content related to this article
- Copyright permission to reproduce figures and/or text from this article

View the Full Text HTML

J|A|C|S
ARTICLES
Published on Web 09/13/2003

Unusual Chemistry of the Complex $Mg^{\bullet+}$(2-Fluoropyridine) Activated by the Photoexcitation of $Mg^{\bullet+}$

Hai-Chuan Liu,[†] Shihe Yang,*[,†] Xin-Hao Zhang,[†] and Yun-Dong Wu*[,†,‡]

Contribution from the Department of Chemistry, The Hong Kong University of Science and Technology, Clear Water Bay, Kowloon, Hong Kong, China, and State Key Lab for Structural Chemistry of Stable and Unstable Species, College of Chemistry, Peking University, Beijing 100871, China

Received June 3, 2003; E-mail: chsyang@ust.hk, chydwu@ust.hk

Abstract: The photochemistry of a gas-phase complex, $Mg^{\bullet+}$(*2*-fluoropyridine), has been studied in the spectral range of ~230−440 nm with a molecular beam coupled with a time-of-flight mass spectrometer. Surprisingly rich chemistry has been observed. Aside from the evaporative photofragment, $Mg^{\bullet+}$, an abundant photoproduct, $C_4H_4^{\bullet+}$, is observed after the electronic excitation of Mg^+. The formation of this photoproduct is associated with the loss of a stable species, CN−Mg−F. Also identified in this work are reactive pathways that occur with the elimination of HCN, HF, or MgF from the complex. The observed photoreactions have been examined in detail using quantum mechanics methods. A distinct structural feature of the complex is the direct attachment of $Mg^{\bullet+}$ to the N atom of fluoropyridine due to the strong electrostatic interaction. The key to the rich photochemistry is the formation of the $FMg^+(C_5H_4N)$ intermediate, through facile fluorine migration. Plausible photoreaction mechanisms have been proposed. These mechanisms account for the evolution of the energized complex with the pre-defined structure en route to the target photoproducts that we have detected.

Introduction

The binding of metal ions to proteins and nucleic acids is crucial to numerous biological functions and dysfunctions of organisms.[1] However, the studies of metal−ligand interactions in organisms are often complicated by the heterogeneity of the system and by the fact that many biologically important metal ions are spectroscopically silent.[1,2] One powerful approach to this problem is to study isolated complexes between metal ions and small molecules that may mimic the binding sites of interest.[3−8] Molecular beam, mass spectrometry, and laser spectroscopy provide important means to study such metal ion−molecule complexes in the gas phase.[9]

During the past few years, we have utilized photodissociation spectroscopy to study the complexes of M^+ (M = alkaline earth metal) and various organic molecules.[10] This has given us important information about the binding modes of the metal ions and dissociation pathways/dynamics of the complexes. For example, $Mg^{\bullet+}$ tends to form π-complexes with benzene and mono-halogen-substituted benzene molecules, although it also favorably attaches to the F atom in fluorobenzene.[10g] For multi-fluoro-substituted benzenes, however, $Mg^{\bullet+}$ favors the association with F atoms rather than π-coordination.[10a] Furthermore, in a complex with pyridine, $Mg^{\bullet+}$ is exclusively linked to the N atom.[10f] Photodissociation of the π-complexes and $Mg^{\bullet+}$-pyridine results mainly in the complex decomposition accompanied by the formation of minor charge-transfer (CT)

[†] Department of Chemistry, The Hong Kong University of Science and Technology.

[‡] State Key Lab for Structural Chemistry of Stable and Unstable Species, College of Chemistry, Peking University.

(1) (a) *Interactions of Metal Ions with Nucleotides, Nucleic Acids and their Constituents*; Sigel, A., Sigel, H., Eds; Metal Ions in Bilogical Systems 32; Marcel Dekker: New York, 1996. (b) *Probing of Nucleic Acids by Metal Ion Complexes of Small Molecules*; Sigel, A., Sigel, H., Eds; Metal Ions in Biological Systems 33; Marcel Dekker: New York, 1996. (c) Dudev, T.; Lim, C. *Chem. Rev.* **2003**, *103*, 773.
(2) Burdette, S. C.; Lippard, S. J. *Proc. Natl. Acad. Sci.* **2003**, 100, 3605.
(3) (a) Rodgers, M. T.; Armentrount, P. B. *J. Am. Chem. Soc.* **2000**, *122*, 8548. (b) Rodgers, M. T.; Armentrount, P. B. *J. Am. Chem. Soc.* **2001**, *124*, 2678.
(4) Russo, N.; Toscano, M.; Grand, A. *J. Am. Chem. Soc.* **2001**, *123*, 10272.
(5) (a) Hoyau, S.; Norrman, K.; McMahon, T. B.; Ohanessian, G. *J. Am. Chem. Soc.* **1999**, *121*, 8864. (b) Hoyau, S.; Ohanessian, G. *J. Am. Chem. Soc.* **1997**, *119*, 2016.
(6) Luna, A.; Amekraz, B.; Tortajada, J.; Morizur, J. P.; Alcami, M.; Mo, O.; Yanez, M. *J. Am. Chem. Soc.* **1998**, *120*, 5411.
(7) (a) Cerda, B. A.; Wesdemiotis, C. *J. Am. Chem. Soc.* **1996**, *118*, 11 884. (b) Cerda, B. A.; Wesdemiotis, C. *J. Am. Chem. Soc.* **1995**, *117*, 9734.
(8) (a) Hu, P. F.; Gross, M. L. *J. Am. Chem. Soc.* **1993**, *115*, 8821. (b) Hu, P. F.; Gross, M. L. *J. Am. Chem. Soc.* **1992**, *114*, 9153. (c) Hu, P. F.; Gross, M. L. *J. Am. Chem. Soc.* **1992**, *114*, 9161. (d) Hu, P. F.; Sorensen, C.; Gross, M. L. *J. Am. Soc. Mass Spectrom.* **1995**, *6*, 1079. (e) Remko, M.; Rode, B. M. *Chem. Phys. Lett.* **2000**, *316*, 489.
(9) (a) Kleiber, P. D.; Chen, J. *Int. Rev. Phys. Chem.* **1998**, *17*, 1. (b) Duncan, M. A. *Annu. Rev. Phys. Chem.* **1997**, *48*, 69. (c) Lu, W.-Y.; Wong, Y. S.; Kleiber, P. D. *J. Chem. Phys.* **2002**, *117*, 6970. (d) Scurlock, C. T.; Pullins, S. H.; Reddic, J. E.; Duncan, M. A. *J. Chem. Phys.* **1996**, *104*, 4591. (e) Misaizu, F.; Sanekata, M.; Fuke, K.; Iwata, S. *J. Chem. Phys.* **1994**, *100*, 1161. (f) Lee, J. I.; Sperry, D. C.; Farrar, J. M. *J. Chem. Phys.* **2001**, 114, 6180. (g) Furuya, A.; Ohshimo, K.; Tsunoyama, H.; Misaizu, F.; Ohno, K.; Watanabe, H. *J. Chem. Phys.* **2003**, *118*, 5456. (h) Armentrout, P. B.; Baer, T. *J. Phys. Chem.* **1996**, *100*, 12866, and references therein. (i) Baer, T.; Hase, W. L. *Organometallic Ion Chemistry*; Freiser, B. S., Ed.; Kluwer Academic Publishers: Dordrecht, 1996.
(10) (a) Liu, H. C.; Wang, C. S.; Guo, W. Y.; Wu, Y.-D.; Yang, S. H. *J. Am. Chem. Soc.* **2002**, *124*, 3794. (b) Yang, X.; Liu, H. C.; Yang, S. H. *J. Chem. Phys.* **2000**, *113*, 3111. (c) Liu, H. C.; Guo, W. Y.; Yang, S. H. *J. Chem. Phys.* **2001**, *115*, 4612. (d) Guo, W. Y.; Liu, H. C.; Yang, S. H. *J. Chem. Phys.* **2002**, *116*, 2896. (e) Guo, W. Y.; Liu, H. C.; Yang, S. H. *J. Chem. Phys.* **2002**, *117*, 6061. (f) Guo, W. Y.; Liu, H. C.; Yang, S. H. *Int. J. Mass Spectrom.* **2003**, *226*, 291. (g) Yang, X.; Gao, K. L.; Liu, H. C.; Yang, S. H. *J. Chem. Phys.* **2000**, *112*, 10 236.

decomposition products. However, starting with complexes characterized by the Mg^+-F linkage also gives rise to abundant photoreaction products.

We emphasize that the photodissociation of the complexes with well-defined structures is initiated by the optical excitation of the unpaired electron in $Mg^{\bullet+}$. The excitation energies are in the ultra-violet spectral range, which not only can cause the decomposition of the complexes but also may activate vicinal covalent bonds and open chemical reaction channels. It is important to realize that such local deposition of electronic energy in a pre-configured complex framework may result in the preferential formation of certain photoproducts.[9,10] In addition to implications to the controlled synthesis of target compounds,[11] this strategy may also have analytical utility for biological molecules by virtue of their characteristic photodissociation patterns.[12]

In the work reported here, we extend the photodissociation study of $Mg^{\bullet+}$(fluorobenzene) and $Mg^{\bullet+}$(pyridine)[10f,g] to the complex of $Mg^{\bullet+}$(*2*-fluoropyridine). What separates *2*-fluoropyridine from both fluorobenzene and pyridine is that it bears both N and F binding sites in close proximity. This unique molecular feature is likely to affect the binding of the metal ion. More importantly, it may engender new photoreactions, such as the formation of a pyridyl cation through MgF elimination, which is isoelectronic to *o*-benzyne,[10a,13] and ring-opening reactions.

As a heterocycle, pyridine (C_5H_5N) is an important biological molecule. It exists in enzymes found in the tissues of all plants and animals [14] and in pharmaceuticals with a wide range of functionalities.[15] Aromatic substitutions may represent a viable strategy in chemotherapy by modifying the biological responses, base-pairing, and ligand−receptor interactions. Indeed, F-substituted pyrimidine such as fluorouracil has been used as a potent drug for inhibiting tumor growth.[16] Moreover, fluorinated molecules, known as fluorometabolites, have been isolated from plants and microorganisms, signaling new developments in biology.[17] Complexes of C_5H_5N with various metal ions have been extensively studied by collision-induced dissociation (CID),[18,19] photolysis,[20] and spectroscopy.[21] However, less attention has been directed to the binding of metal ions to substituted pyridines.[19] In our studies of $Mg^{\bullet+}$(*2*-fluoropyridine), we combine photodissociation experiments (230−440 nm) and comprehensive quantum mechanics calculations. Some unusual photoreaction patterns of the complex have been identified and rationalized by tracing the transition state structures and intermediates.

Experiments and Computations

Photodissociation Experiments. Because the main cluster apparatus has been described elsewhere,[10] only a brief description relevant to the present experiment is given here. A rotating magnesium rod (5 mm in diameter and 5 cm in length) was mounted 15 mm downstream from the exit of a pulsed valve (General Valve). The sample rod was rotated and translated simultaneously by a step motor on each laser pulse to expose fresh surfaces during the laser-ablation experiments. The pulsed valve was employed to generate beams of *2*-fluoropyridine by supersonic expansion of the vapor seeded in helium with a backing pressure of ~40 psi through a 0.5 mm diameter orifice. The second harmonic (532 nm) of a Nd:YAG laser (~40 mJ/pulse) was weakly focused on a ~1 mm diameter spot of the magnesium disk for the generation of metal cations. The laser-produced species containing metal ions and atoms traversed perpendicularly to the supersonic jet stream 20 mm from the ablation sample target, forming a series of metal cations solvated by *2*-fluoropyridine. The nascent complexes and clusters then traveled 14 cm downstream to the extraction region of the reflectron time-of-flight mass spectrometer (RTOFMS).

The cation−molecule complexes were accelerated vertically by a high voltage pulse in a two-stage extractor. After extraction, the cluster cations were steered by a pair of horizontal plates and a pair of vertical deflection plates. All of the cluster cations were reflected by the reflectron and finally detected by a dual-plate microchannel plate detector (MCP). In the photodissociation experiments, a two-plate mass gate equipped with a high-voltage pulser was used to select the desired cluster cations. The mass-selected cluster cations, once at the turn-around region of the reflectron, were irradiated with a collimated beam of a dye laser for photolysis. The parent and nascent daughter cations were reaccelerated by the reflectron electric field and detected by the MCP detector. The dye laser was pumped by a XeCl excimer laser (Lambda-Physik LPX210i/LPD3002). The laser dyes *p*-terphenyl, DMQ, BBQ, Stilbene 1, and Coumarin 440 were used to cover the spectral region of 335−450 nm, while the second harmonic with Coumarin 503 and Coumarin 480 spanned the spectral region of 230−270 nm. The branching fractions of each fragment were obtained from the corresponding photodissociation difference mass spectra at different wavelengths. Assignments of mass spectra were accomplished by careful least-squares fitting, which could distinguish one mass unit in the mass range of our study.

Computational Details. Because the geometries of the photofragments in MS were unknown, a *backtracking methodology* was employed: (1) Various possible isomeric structures of each fragment were searched and compared with the experimental conditions to determine the most likely candidates; (2) reaction pathways were designed for each isomeric structure and studied in detail.

Quantum mechanics calculations were performed by the GAUSSIAN 98 program.[22] The observed photoreactions, although initiated by electronic excitation, were assumed to occur on the ground-state surface after internal conversion. All species were calculated with the density functional theory B3LYP method[23] using the 6-31+G** basis set. Each stationary point was characterized by vibrational frequency analysis

(11) Shin, S. L.; Chen, Y.; Nicholaisen, S.; Sharpe, S. W.; Beaudet, R. A.; Wittig, C. *Adv. Photochem.* **1991**, *16*, 249.
(12) Senko, M. W.; Speir, J. P.; McLafferty, F. W. *Anal. Chem.* **1994**, *66*, 1866.
(13) (a) Hoffman, R. W. *Dehydrobenzene and Cycloalkynes;* Academic Press: New York, 1967. (b) Heaney, H. *Chem. Rev.* **1962**, *62*, 81. (c) Sander, W. *Acc. Chem. Res.* **1991**, *24*, 669. (d) Wenthold, P. G.; Squires, R. R. *J. Am. Chem. Soc.* **1994**, *116*, 6401. (e) Kenttamaa, H. I. *J. Chem. Soc. Perkin Trans.* 2, **1999**, 2233. (f) Jiao, H. J.; Schleyer, P. v. R.; Beno, B. R.; Houk, K. N.; Warmuth, R. *Angew. Chem., Int. Ed. Engl.* **1997**, *36*, 2761. (g) Borden, W. T. *Diradicals;* Wiley: New York, 1982.
(14) Brody, F.; Ruby, P. R. *Heterocyclic Compounds*; Klingsberg E., Ed; Pyridine and Derivatives, Part 1; Interscience Publishers: New York, 1960; pp 99.
(15) (a) Coutts, R. T.; Casy, A. F. *Pyridine and Its Deravatives;* Abramovitch R. A., Ed; Suppl., Part 4; John & Sons: New York, 1975; p 445. (b) Gilchrist, T. L. *Heterocyclic Chemistry*, 3rd ed.; Longman Singapore Publisher Inc.: Singapore, 1997; p 125.
(16) (a) Heidelberg, C. *Cancer Medicine*, 2nd ed.; Holland, J. F., Frei, E., Eds; Lea & Febiger: Philadelphia, 1982; p 801. (b) Chabner, B. A. *Pharmacologic Principles of Cancer Treatment;* Chamber, B. A., Ed; Saunders: Philadelphia, 1982; p 340.
(17) See, for example, *Biohalogenation*, Neidleman, S. L.; Geigert, J., Ed; Ellis Horwood Limited: Chichester, 1986.
(18) Rodgers, M. T.; Stanely, J. R.; Amunugama, R. *J. Am. Chem. Soc.* **2000**, *122*, 10969.
(19) (a) Rodgers, M. T. *J. Phys. Chem. A* **2001**, *105*, 8145. (b) Rodgers, M. T. *J. Phys. Chem. A* **2001**, *105*, 2374. (c) Amunugama, R.; Rodgers, M. T. *J. Phys. Chem. A* **2001**, *105*, 9883.
(20) (a) Yang, Y.-S.; Hsu, W.-Y.; Lee, H.-F.; Huang, Y.-C.; Yeh, C.-S.; Hu, C.-H. *J. Phys. Chem. A* **1999**, *103*, 11287. (b) Hsu, W.-Y.; Lee, H.-F.; Lai, C.-C.; Su, P.-H.; Yeh, C.-S. *New J. Chem.* **2002**, *26*, 481.
(21) (a) Puskar, L.; Stace, A. J. *J. Chem. Phys.* **2001**, *114*, 6499. (b) Walker, N.; Dobson, M. P.; Wright, R. R.; Barran, P. E.; Murrell, J. N.; Stace, A. J. *J. Am. Chem. Soc.* **2000**, *122*, 11138. (c) Puskar, L.; Barran, P. E.; Wright, R. R.; Kirkwood, D. A.; Stace, A. J. *J. Chem. Phys.* **2000**, *112*, 7751. (d) Walker, N.; Wright, R. R.; Stace, A. J. *J. Am. Chem. Soc.* **1999**, *121*, 4837.

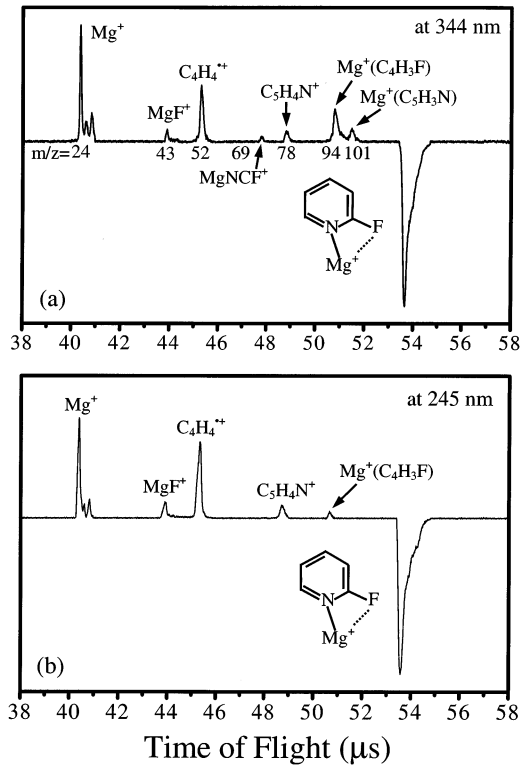

Figure 1. Photodissociation difference mass spectra of the complex $Mg^{\bullet+}$-(2-fluoropyridine) at 344 nm (a) and at 245 nm (b).

(minimum with zero; transition structure with one imaginary frequency). To confirm the transition structures for some key reaction pathways, intrinsic reaction coordinate (IRC) calculations were used to follow the reaction pathways. All of the relative energies are reported with the corrections of zero-point energy (ZPE). It should be cautioned that the use of the DFT/B3LYP method often encounters problems in dealing with radical cations.[24] Higher-level calculations such as CCSD(T) would be desirable to get more accurate results. However, we did not do this because we are only interested in understanding the reaction pathways based on the experimentally observed products.

The vertical excitation energies and corresponding oscillator strengths of the $Mg^{\bullet+}$(2-F-pyridine) complex were calculated with the CIS/6-31+G** method on the B3LYP/6-31+G** geometry.

Results and Discussion

A. Wavelength-Resolved Photodissociation at 230−440 nm. Figure 1 presents the photodissociation difference mass spectra of $Mg^{\bullet+}$(2-F−C_5H_4N) at short (245 nm, 5.06 eV) and long (344 nm, 3.60 eV) wavelengths. The disappearance of $Mg^{\bullet+}$(2-F−pyridine) is coupled with the appearance of several positively charged species. The main features are summarized as follows: (1) At both photon energies, $Mg^{\bullet+}$ is the major photofragment, which can be considered as the evaporation from $Mg^{\bullet+}$(2-F−C_5H_4N) upon electronic excitation. (2) In both cases, MgF^+ and $C_5H_4N^+$ appear as minor photoproducts. Each can be regarded as being from one of the two fragmentation modes of MgF^+(C_5H_4N), that is, the elimination of MgF^+ or MgF. It is interesting that the two peaks are nearly identical in intensity and that, at $h\nu = 5.06$ eV, the relative intensities of the two peaks are slightly higher than those at $h\nu = 3.60$ eV. (3) The second most abundant photoproduct cation has a mass unit of 52 at both photon energies. It can be designated $C_4H_4^{\bullet+}$ which is formed by CN−Mg−F elimination. Although this peak could also be assigned to $C_3H_2N^+$ partnered with C_2H_2 and MgF, it would be difficult to posit a proper mechanism for its formation according to our calculations (see below). (4) The peak at $m/z = 94$ can be assigned to Mg^+(C_4H_3F), which corresponds to the elimination of HCN. The elimination of HCN is dominant in the photodissociation of pyridine.[25] Interestingly, the higher yield of this photoproduct at $h\nu = 3.60$ eV seems to be correlated with the reduced yield of $C_4H_4^{\bullet+}$. (5) Two more minor photoproducts are observed at $h\nu = 3.60$ eV: a very small peak of CN−MgF^+ and a moderate peak of Mg^+(C_5H_3N). The formation of the two photoproducts corresponds to the elimination of neutral C_4H_4 and HF, respectively.

It is noteworthy that the observed rich photoinduced reaction patterns for $Mg^{\bullet+}$(2-F−C_5H_4N) are the direct result of fluorine substitution. In the absence of F-substitution, only a weak CT photoproduct was observed.[10f] CID experiments of $Mg^{\bullet+}$-(pyridine) resulted in the only product of $Mg^{\bullet+}$.[18] In another photolysis study of M^+(pyridine) (M = Cu, Ag, and Au), the charge-transfer product of pyridine$^{\bullet+}$ was observed exclusively.[20] However, a single F-substitution next to N leads to extensive photoinduced ring-opening reactions, most likely triggered by the breakage of the C−F bond.

Shown in Figure 2a are action spectra of the photofragments from $Mg^{\bullet+}$(2-F−C_5H_4N) in the wavelength ranges of ∼230−270 nm and ∼330−440 nm. No spectral features have been identified in the region of ∼270−330 nm. Clearly, the electronic transitions of $Mg^{\bullet+}$ ($3^2P \leftarrow 3^2S$) have been split to a relatively sharp peak at 242 nm and a broader peak at 356 nm with a shoulder at 375 nm and a rather long tail at the red. The blue-shifted features in the action spectra are attributed to the promotion of the *s* electron of $Mg^{\bullet+}$ to the p_z orbital, which interacts repulsively with the lone pair electrons of the N atom. The red-shifted peaks are due to the population of the p_x and p_y orbitals of $Mg^{\bullet+}$. The action spectra of the complex are consistent with the CIS calculations in both the peak position and intensity (see Figure 2), which supports the complex structure in which $Mg^{\bullet+}$ is linked to the N atom. There is a long tail above 380 nm in the action spectra. This may be caused by the excitation of the CT state, which is quenched by the back CT, followed by the ground-state decomposition. It is worth mentioning that the action spectra of the reactive photoproducts are analogous to the action spectrum of $Mg^{\bullet+}$. This indicates that the reactions are initiated by photoexcitation

(22) Frisch, M. J.; Trucks, G. W.; Schlegel, H. B.; Scuseria, G. E.; Robb, M.A.; Cheeseman, J. R.; Zakrzewski, V. G.; Montgomery, J. A., Jr,; Stratmann, R. E.; Burant, J. C.; Dapprich, S.; Millam, J. M.; Daniels, A. D.; Kudin, K. N.; Strain, M. C.; Farkas, O.; Tomasi, J.; Barone, V.; Cossi, M.; Cammi, R.; Mennucci, B.; Pomelli, C.; Adamo, C.; Clifford, S.; Ochterski, J.; Petersson, G. A.; Ayala, P. Y.; Cui, Q.; Morokuma, K.; Malick, D. K.; Rabuck, A. D.; Raghavachari, K.; Foresman, J. B.; Cioslowski, J.; Ortiz, J. V.; Baboul, A. G.; Stefanov, B. B.; Liu, G.; Liashenko, A.; Piskorz, P.; Komaromi, I.; Gomperts, R.; Martin, R. L.; Fox, D. J.; Keith, T.; Al-Laham, M. A.; Peng, C. Y.; Nanayakkara, A.; Gonzalez, C.; Challacombe, M.; Gill, P. M. W.; Johnson, B. G.; Chen, W.; Wong, M. W.; Andres, J. L.; Gonzalez, C.; Head-Gordon, M.; Replogle, E. S.; Pople, J. A. *Gaussian 98*, Revision A.7; Gaussian, Inc.: Pittsburgh, PA, 1998.
(23) (a) Becke, A. D. *J. Chem. Phys.* **1993**, *98*, 5648. (b) Lee, C.; Yang, W.; Parr, R. G. *Phys. Rev. B* **1988**, *37*, 785.
(24) (a) Bally, T.; Sastry, G. N. *J. Phys. Chem. A* **1997**, *101*, 7923. (b) Crawford, T. D.; Kraka, E.; Stanton, J. F.; Cremer, D. *J. Chem. Phys.* **2001**, *114*, 10 638. (c) Braida, B.; Lauvergnat, D.; Hiberty, P. C. *J. Chem. Phys.* **2001**, *115*, 90. (d) Koga, N.; Morokuma, K. *J. Am. Chem. Soc.* **1991**, *113*, 1907. (e) Galbraith, J. M.; Schreiner, P. R.; Harris, N.; Wei, W.; Wittkopp, A.; Shaik, S. *Chem. Eur. J.* **2000**, *6*, 1446. (f) Grafenstein, J.; Hjerpe, A. M.; Kraka, E.; Cremer, D. *J. Phys. Chem. A* **2000**, *104*, 1748. (g) Kraka, E.; Anglada, J.; Hjerpe, A.; Filatov, M.; Cremer, D. *Chem. Phys. Lett.* **2001**, *348*, 115.
(25) Prather, K. A.; Lee, Y. T. *Isr. J. Chem.* **1994**, *34*, 43.

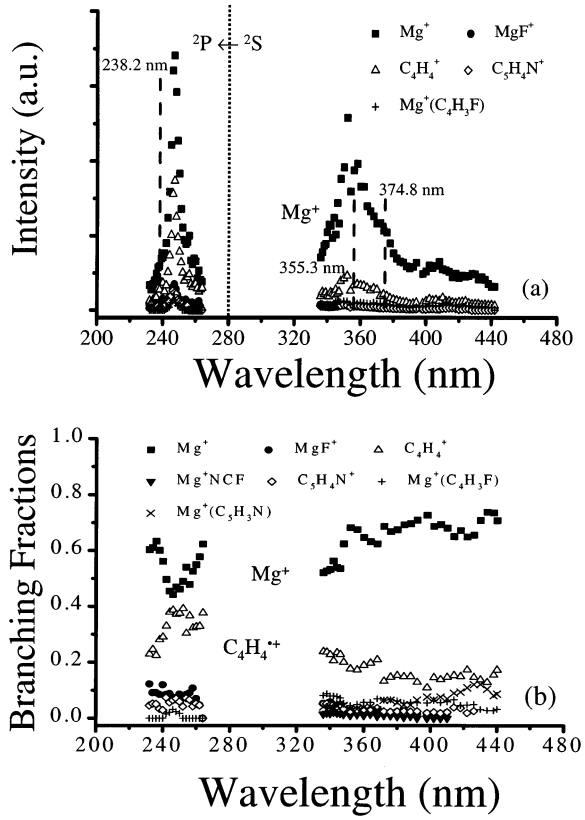

Figure 2. (a) Action spectra of the complex $Mg^{\bullet+}$(2-fluoropyridine). The vertical axis represents the relative yields of the photofragments. The dotted line indicates the atomic transition of $Mg^{\bullet+}$ ($3^2P \leftarrow 3^2S$) at 280 nm. The dashed lines denote the calculated absorption spectra using the CIS method. (b) Branching fraction curves of $Mg^{\bullet+}$(2-fluoropyridine).

of the unpaired 3*s* electron of Mg^+ rather than the $\pi \rightarrow p^*$ transitions of the substituted pyridines.[26]

The branching fraction curves for the photodissociation of $Mg^{\bullet+}$(2-F−C_5H_4N) in the wavelength ranges of ∼230−270 nm and ∼330−440 nm are plotted in Figure 2b. The branching fraction of $Mg^{\bullet+}$ is in the range of ∼0.5−0.8. The branching fraction of $C_4H_4^{\bullet+}$ increases gradually from ∼0.1 at 440 nm to ∼0.4 at 240 nm and then drops down steadily to ∼0.2 at 230 nm. It is interesting to note that the branching fraction curves of $C_4H_4^{\bullet+}$ and $Mg^{\bullet+}$ are anti-correlated, suggesting a competition of the two branching pathways.

B. Structural and Energetic Analysis of the Parent Complex and Photoproducts. As the first step of our theoretical study, possible structures of the $Mg^{\bullet+}$(2-F−C_5H_4N) (**1**) complex and the corresponding photoproducts (**P1**−**P7**) were searched in depth with full geometrical optimization at the B3LYP/6-31+G** level. Although all calculated photoproducts are given in Figure S1 of the Supporting Information (SI), Figure 3 summarizes the key calculation results.

Although $Mg^{\bullet+}-\pi$ and $Mg^{\bullet+}$−F bindings are conceivable, the most stable structure of the complex is characterized by the linkage of $Mg^{\bullet+}$ to the N atom. Attempts made to locate the stable $Mg^{\bullet+}-\pi$ and $Mg^{\bullet+}$−F bindings complexes always resulted in the energetically favorable $Mg^{\bullet+}$−N binding complex. The binding is much the same as in $Mg^{\bullet+}$−pyridine except that here $Mg^{\bullet+}$ interacts attractively with the neighboring F atom,

Table 1. Calculated Relative Energies (eV) for the Formation of P2 and P3 by Elimination of $^{\bullet}MgF$ and ^{+}MgF from the $^{+}MgF(C_5H_4N)$ Isomeric Intermediates[a]

isomeric intermediates		- ^{+}MgF		- $^{\bullet}MgF$	
		BDE	P2	BDE	P3
I-1	0.13	3.07	3.20	2.75	2.88
I-2a	1.36	3.31	4.67	1.48	2.88[b]
I-2b	0.51	3.33	3.84	3.42	3.93
I-2c	1.66	3.13	4.79	2.27	3.93[c]
I-3a	0.34	3.07	3.41	3.28	3.62
I-3b	1.58	3.53	5.11	2.04	3.62[d]
I-3c	1.29	3.10	4.39	3.53	4.82

[a] The geometries of $C_5H_4N^{\bullet}$ and $C_5H_4N^+$ species are similar to those in the corresponding $^{+}MgF(C_5H_4N)$ intermediates unless otherwise noted. [b] Same as the product from I-1. [c] Same as the product from I-2b. [d] Same as the product from I-3a.

resulting in a 11.1° angular deviation (Figure 4) from the symmetry axis of 2-F−C_5H_4N.[10f,18−21,27] The bond dissociation energy (BDE) of $Mg^{\bullet+}$(2-F−C_5H_4N) (**1**) is calculated to be 1.91 eV (see Figure 3, **P1**). The calculated BDE is slightly smaller than that of $Mg^{\bullet+}(C_5H_5N)$ (2.08 eV)[10f] but still larger than the BDEs of alkali metal ion-pyridine complexes (1.88, 1.31, and 0.94 eV for Li^+, Na^+, and K^+, respectively).[18] This indicates that the $Mg^{\bullet+}$(2-F−C_5H_4N) complex has some covalent character in addition to the dominant electrostatic interaction, due to (1) the reduced Pauli repulsion arising from the sp-polarization of $Mg^{\bullet+}$ and (2) the conjugation of the π-orbitals of 2-F−C_5H_4N with the 3p orbital of $Mg^{\bullet+}$.

For the formation of **P2** and **P3**, calculations indicate that the elimination of MgF^+ and MgF from **1** costs about 3.20 and 2.88 eV, respectively, suggesting that both processes can be achieved with the photon energies used in the experiment. As will be discussed later and shown in Table 1, the cyclic forms of $C_5H_4N^+$ and C_5H_4N shown in Figure 3 are more stable than all the ring-opened isomers. Gozzo and Eberlin have studied the *o*-pyridyl cation theoretically and experimentally [28,29] and found it to be very stable compared with the *m*- and *p*- pyridyl cations. Our calculations give similar results.

For the radical cation $C_4H_4^{\bullet+}$ (**P5**), a total of five isomers were studied. The three most stable structures are shown in Figure 3. Although the methylene cyclopropene radical cation (**A**) is the most stable, consistent with the prediction by Bally et al. using a different method,[30] the open form and cyclobutadiene radical cation are about 0.30−0.40 eV less stable. This suggests that the pathways for the formation of these structures should all be explored. We attribute the $m/z = 52$ peak to $C_4H_4^{\bullet+}$ rather than $C_3H_2N^+$ on the basis of the energetic consideration. It takes about 5.85 eV, which is higher than the photon energies we used, to form the photoproduct of $C_3H_2N^+$ associated with the loss of C_2H_2 and MgF.

Two candidate structures of $Mg^+(C_5H_3N)$ (**P7**) resulting from the loss of HF from $Mg^{\bullet+}$(2-F−C_5H_4N) were calculated. It requires about 2.66 eV to generate the open form **A**,[31] but the cyclic structure (**B**) derived from direct elimination of HF from **1** requires an energy of 4.38 eV. Therefore, with the photon energy of 3.60 eV, only **A** is formed.

(26) (a) Medhi, K. C.; Medhi, R. N. *Spectrochim. Acta* **1990**, *46*, 1169. (b) Medhi, K. C.; Medhi, R. N. *Spectrochim. Acta* **1990**, *46*, 1333.
(27) Stockigt, D. *J. Phys. Chem. A* **1997**, *101*, 3800.
(28) (a) Carvalho, M.; Gozzo, F. C.; Mendes, M. A. Sparrapan, R.; Kascheres, C.; Eberlin, M. N. *Chem. Eur. J.* **1998**, *4*, 1161. (b) Gozzo, F. C.; Eberlin, M. N. *J. Org. Chem.* **1999**, *64*, 2188.
(29) Kauffmann, T. *Angew. Chem., Int. Ed. Engl.* **1965**, *4*, 543.
(30) Hrouda, V.; Roeselova, M. R.; Bally, T. *J. Phys. Chem. A* **1997**, *101*, 3925.

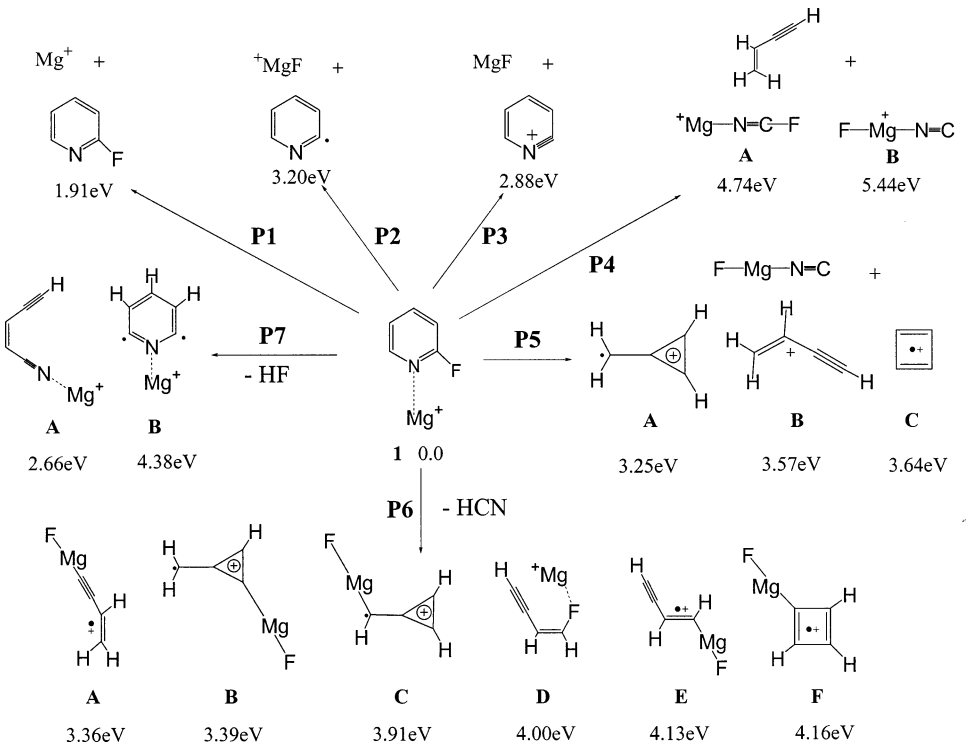

Figure 3. Possible structures for the selected products from photodissociation of $Mg^{\bullet+}(2\text{-}F{-}C_5H_4N)$. The calculated relative energies are at the B3LYP/6-31+G** level.

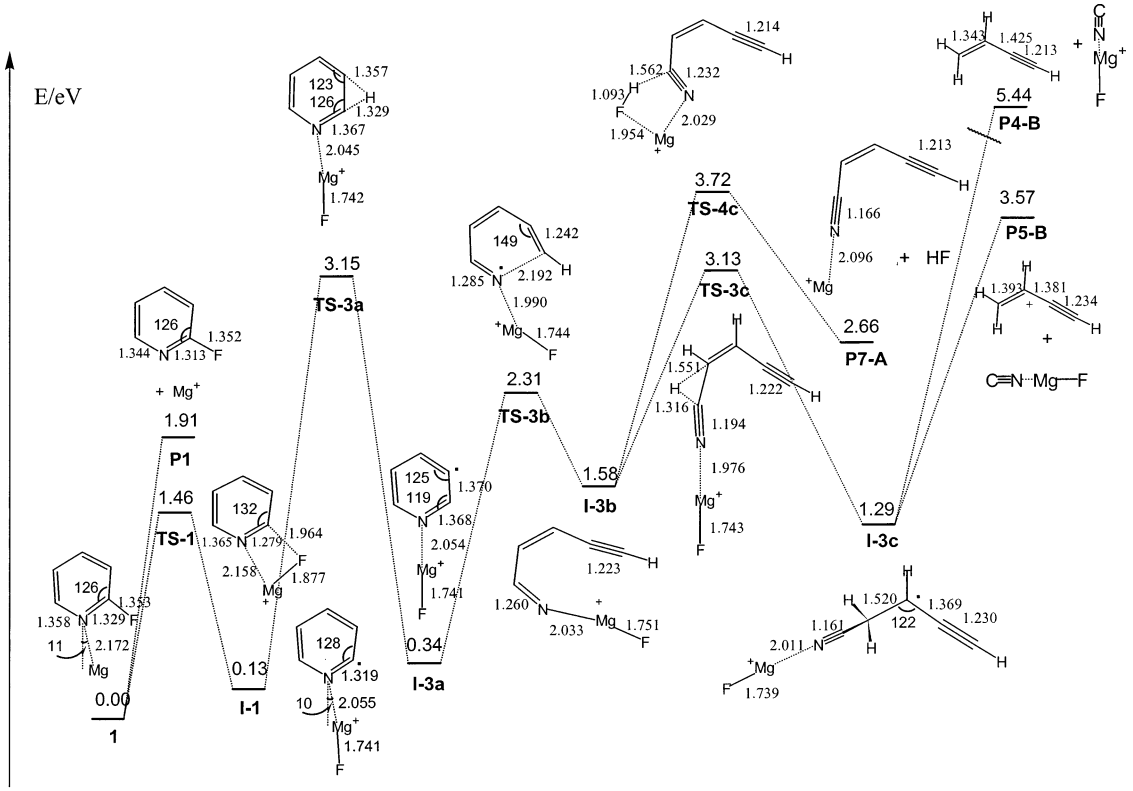

Figure 4. Schematic energetic representation of the photoreaction channels leading to **P1**, **P4-B**, **P5-B**, and **P7-A**. Bond lengths are in angstroms and bond angles are in degrees.

A total of 15 structures were examined for $Mg^+(C_4H_3F)$ (**P6**). Shown in Figure 3 are six of the representative structures. The other nine structures, which are given in the SI, are less stable. The most stable structures are found to be **A** and **B.** We predict that these two structures are energetically accessible with our laser light sources. Other structures cannot be generated by the 3.60 eV photons and, therefore, the mechanisms for the formation of those species were not explored in detail.

C. Isomerization of the $MgF^+(C_5H_4N)$ Intermediate. On the basis of the above calculations, the likely reaction pathways were designed for each observed photoproduct. The calculated reaction pathways and potential energy profiles are shown in

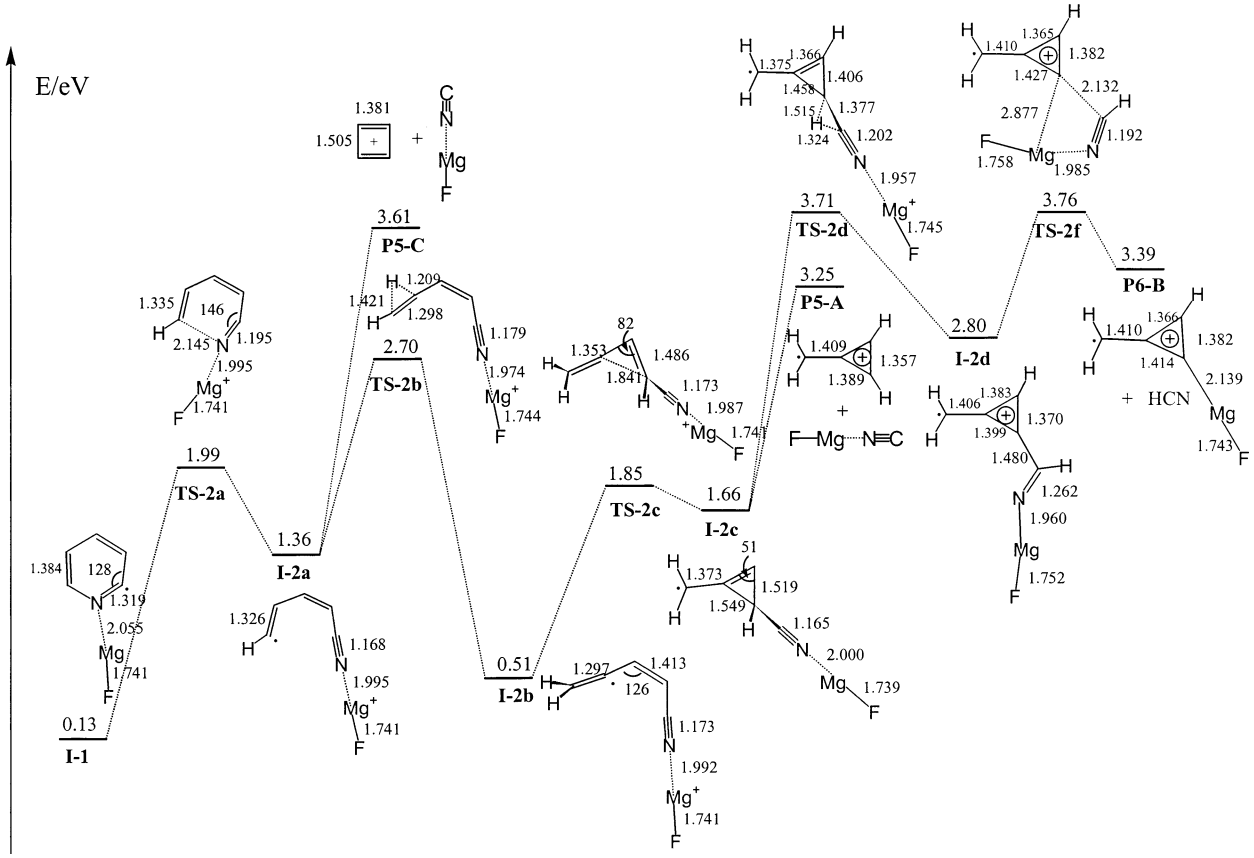

Figure 5. Schematic energetic representation of the reaction channels leading to **P5-A**, **P5-C** and **P6-B**. Bond lengths are in angstroms and bond angles in degrees.

Figures 4 and 5. The structural drawings were converted from calculated three-dimensional geometries and selected geometrical parameters are given. The calculated atomic charges and atomic spin densities of the transition structures and intermediates are provided in the SI (Figure S2). Some less likely pathways that have been investigated are also presented in Figure S3 of the SI.

As shown in Figure 4, although the dissociation of Mg^+ from **1** is an easy process with an energy of about 1.91 eV, fluorine migration to form **I-1** is even easier, with a barrier of about 1.46 eV. Transition structure **TS-1** has a four-centered geometry with the C−F bond (1.964 Å) considerably broken and the Mg−F bond (1.877 Å) considerably formed. Because of the ring constraint, the Mg atom has to deviate further from the pyridine symmetry axis. The intermediate **I-1** is calculated to be only slightly (0.20 eV) less stable than **1**. The easy formation of **I-1**, which bears a radical center at C2, is the key to the rich photochemistry. For the $Mg^{\bullet+}(C_5H_5N)$ complex, a similar hydrogen migration would encounter a barrier of 2.66 eV, leading to an unstable intermediate $MgH^+(C_5H_4N)$ (1.99 eV).

Our calculations indicate that with the energy provided by photon absorption, the $MgF^+(C_5H_4N)$ **I-1** can be converted into various isomers through two pathways. In the first pathway, a 1,2-hydrogen shift reaction occurs. Because the positive charge is located on Mg and the radical is on the ring, it is a hydrogen atom shift. The hydrogen migrates from C2 to C3 in the pyridine ring plane (**TS-3a**). The calculated activation energy, 3.02 eV, is higher than that of proton shifts in a phenyl cation,[32] but it is similar to those in benzyne.[33] The resulting intermediate, **I-3a**, is only about 0.20 eV less stable than **I-1**. **I-3a** can undergo ring-opening through **TS-3b** to form **I-3b**. **I-3b**, in which the Mg atom tilts toward the terminal triple bond to gain some stabilization, undergoes another hydrogen shift through transition structure **TS-3c** to form intermediate **I-3c.** The calculated activation energy for this 1,2-hydrogen shift is about 1.55 eV, much lower than that for **TS-3a**. **TS-3c** is a π-assisted hydrogen shift transition structure, whereas **TS-3a** is a pure σ-hydrogen shift transition structure.

The second pathway of isomerization, which is shown in Figure 5, is the direct N1−C6 bond breaking in **I-1** to form intermediate **I-2a**. It is noted that the barriers for **TS-2a** and **TS-3b** are quite similar, close to 2 eV. **I-2a** can also undergo a facile 1,2-hydrogen shift to form a more stable intermediate **I-2b**. This is because **I-2a** is a σ-radical, while the radical in **I-2b** is stabilized by π-conjugation. **I-2b** can be further converted into a cyclopropene intermediate **I-2c**, which can undergo a 1,2-hydrogen shift to form intermediate **I-2d**.

D. Rationalization of the Photoproduct Formation. Formation of P2 (MgF^+ and C_5H_4N) and P3 (MgF and $C_5H_4N^+$). In principle, **P2** and **P3** can be formed from each isomer of $MgF^+(C_5H_4N)$. The calculated relative energies of these isomers as well as the corresponding **P2** and **P3** derived from these isomers with respect to **1** are collected in Table 1. Examination of Table 1 indicates that **I-1** is not only the most stable, but

(31) The trans-form is calculated to be about 1 kcal/mol more stable than **A**, which central double bond is in the cis form. However, the trans form is difficult to achieve.

(32) (a) Schleyer, P. v. R.; Kos, A. J.; Raghavachari, K. *J. Chem. Soc., Chem. Commun*. **1983**, 1296. (b) Ignatyev, I. S.; Sundius, T. *Chem. Phys. Lett*. **2000**, *326*, 101.

(33) Diau, E. W.-G.; Casanova, J.; Roberts, J. D.; Zewail, A. H. *Proc. Nat. Aca. Sci*. **2000**, *97*, 1376.

also results in the most stable structures of **P2** and **P3**, which are cyclic. In addition, except for **I-1**, the dissociation of either MgF^+ or MgF from each isomer requires a higher energy than the immediate reaction shown in Figures 4 and 5. It can be concluded that **P2** and **P3** are formed mainly from direct dissociation of **I-1**. This is also in agreement with the experimental observation that the yields of the two products are nearly independent of the photon energies.

The energy needed for the formation of MgF^+ with $C_5H_4N^{\bullet}$ is calculated to be 3.20 eV. MgF^+ is only detectable at wavelengths shorter than ~410 nm (3.02 eV) from the photolysis of Mg^+(2-F$-C_5H_4N$) (see Figure 2b). This threshold value can be regarded as the appearance potential (AP) of MgF^+ from the parent complex, which agrees well with the calculated value. The appearance potential for $C_5H_4N^+$ with MgF (**P3**) (see Figure 2) can be roughly determined to be ~420 nm (2.95 eV), which is also close to the calculated value of 2.88 eV.

Formation of P5 ($C_4H_4^{\bullet+}$ and CN−Mg−F) and P-6 (Mg^+-(C_4H_3F) and HCN). There are three pathways for the formation of $C_4H_4^{\bullet+}$. The main pathway is the formation of **P5-A** from intermediate **I-2c** (Figure 5). The formations of **P5-B** from **I-3c** (Figure 4) and of **P5-C** from **I-2a** (Figure 5) are less favorable and are likely inaccessible with photons of 3.60 eV but accessible for $h\nu = 5.06$ eV.

The formation of $Mg^+(C_4H_3F)$ (**P6-B**) (Figure 5) shares the same pathway as the formation of **P5-A**, both being from intermediate **I-2c**. The calculated energies of **TS-2d** and **TS-2f** are somewhat higher than the photon energy at 344 nm (3.60 eV) by about 2 kcal/mol. This is probably due to the inaccuracy of the calculation method. Because all our effort to find another pathway with a lower barrier for the formation of **P6** failed (See Figure S3 of the SI), this pathway is probably most close to the truth. The formation of **P5-A** and **P6-B** is competitive and the formation of **P5-A** is energetically more favorable, which is in agreement with the experimental observation that the yield of $C_4H_4^{\bullet+}$ is higher than that of $Mg^+(C_4H_3F)$ (Figure 1a) for 3.60 eV photons. In addition, when more energetic photons (5.06 eV) are used, the elevated energy would allow the formation of **P5-B** and **P5-C** but no additional channel would be possible for the formation of **P6**. As a result, the yield of **P5** is expected to increase, whereas the chance for the formation of **P6**, which competes with the formation of **P5**, is reduced. This is in accord with the experimental observation that, at photon energies of 5.06 eV, the yield of $C_4H_4^{\bullet+}$ (**P5**) is increased while the yield of $Mg^+(C_4H_3F)$ (**P6**) is reduced (Figure 1b).

Formation of P4 ($CN-MgF^+$ and C_4H_4) and P7 (Mg^+-(C_5H_3N) and HF). The formation of **P4** can be achieved from **I-3c**. This leads to the formation of **P4-B** and requires an overall energy of about 5.44 eV from **1**. The photon energy at 245 nm (5.06 eV) is not enough. However, with two-photon excitation at 344 nm (7.20 eV), the dissociation reaction can occur. This is in agreement with the experimental observation that the formation of $CN-MgF^+$ is observed only at 344 nm, albeit with a very low yield.[34]

It is also interesting to point out that $F-CN-Mg^+$ (Figure 3, **P4-A**) is more stable than $CN-MgF^+$ (**P4-B**) by about 0.70 eV. If **P4-A** were formed, it would have been observed at the photon energy of 5.06 eV. However, our calculations indicate that there is no accessible reaction channel for the formation of this species, in agreement with the experimental result.

The calculations indicate that the formation of $Mg^+(C_5H_3N)$ (**P7**) is energetically allowed at both $h\nu = 3.60$ eV and $h\nu = 5.06$ eV.[35] Further loss of $Mg^{\bullet+}$ from **P7** requires an overall energy of 4.75 eV with respect to **1**. Therefore, at $h\nu = 5.06$ eV, calculations suggest that $Mg^+(C_5H_3N)$ should further dissociate into $Mg^{\bullet+}$ and C_5H_3N. This is in agreement with the experimental observation that $Mg^+(C_5H_3N)$ is observed only at $h\nu = 3.60$ eV.

Conclusion

In summary, the ultraviolet photochemistry of the complex $Mg^{\bullet+}$(2-F$-C_5H_4N$) triggered by the electronic excitation of $Mg^{\bullet+}$ has been found to be remarkably rich. The combination of photodissociation spectroscopy and quantum mechanics calculations has revealed the photoreaction pathways. The key reason for the rich photochemistry is the facile formation of the $FMg^+(C_5H_4N)$ intermediate, **1**, through fluorine migration, which can be converted into various isomeric forms. The primary driving force for the photoproduction of $C_4H_4^{\bullet+}$, which can be generated in several forms, is the formation of the energy-sink molecule, CN−Mg−F. Some minor photoproducts such as $C_5H_4N^+$, $Mg^+(C_4H_3F)$, and $Mg^+(C_5H_3N)$ are also produced by the loss of MgF, HCN, and HF molecules, respectively. Several neutral photoproducts, such as C_5H_4N and C_5H_3N, which correspond to the loss of MgF^+, $Mg^{\bullet+}$ plus HF, are also possible.

Acknowledgment. We are grateful to the Research Grants Council of Hong Kong for financial support of this research.

Supporting Information Available: Calculated photoproducts (Figure S1), geometries, relative energies, charge distributions, and spin densities (Figure S2), and less likely pathways for product formation (Figure S3). This material is available free of charge via the Internet at http://pubs.acs.org.

JA036476A

(34) In principle, a two-photon process at 245 nm (7.20 eV) would also lead to the formation of **P4-B**. However, the laser light intensity in our experiment was much weaker at 245 nm than at 344 nm, which made the two-photon process much less likely.

(35) As shown in the SI (Figure S3. (d)), HF elimination from **I-1** requires at least 4.38 eV, which is unfavorable compared to that from **I-3b**.